Indian Journal of Pure & Applied Physics
Vol. 62, October 2024, pp. 911-917
DOI: 10.56042/ijpap.v62i10.11584

Design and Analysis of One Port SAW Multi-layered Resonator by Reducing Return Loss of the Device

Baruna Kumar Turuk & Basudeba Behera*

Department of Electronics and Communication, National Institute of Technology, Jamshedpur, Jharkhand 831 014, India

Received 3 June 2024; accepted 4 September 2024

This work comprehensively investigates the design and analysis of one-port multilayer surface acoustic wave (SAW) resonators, focusing on their application in communication systems. The motivation behind this work stems from the increasing demand for high-performance communication systems with minimal signal loss. Return loss, a key parameter in evaluating signal integrity, directly impacts the efficiency and reliability of communication systems. The methodology involves a systematic design process, starting with selecting suitable materials for the multilayer structure based on their acoustic properties and compatibility with communication frequencies. The finite element simulation tool is utilized to model and simulate the SAW resonator's behaviour, allowing for precise optimization of design parameters such as layer thickness, electrode configuration, and interdigital transducer (IDT) design. Various performance metrics, including return loss, bandwidth, and quality factor, are evaluated to assess the effectiveness of the resonator in minimizing signal reflections. The results show significant improvements in return loss reduction, demonstrating the effectiveness of the proposed design approach. This work optimised the height of the electrode and found the insertion loss of the proposed device, which was-27dB. The proposed device demonstrates enhanced performance characteristics suitable for various communication system applications, including wireless networks, radar systems, and satellite communications.

Keywords: Interdigital transducer; Surface acoustic wave; Return loss; Q-factor

1 Introduction

The surface acoustic wave (SAW) device is a micromechanical electronic device that processes signals. The SAW devices were initially utilised as an IF filter for TV; however, since it is found widespread application in a variety of technological applications, such as radio frequency filters[1], wireless communication systems, gas sensors, radio frequency tags[2], sensors for biomolecules[3,4], chemical sensors[5,6], and Regarding mobile communication applications, the application of SAW devices in radio frequency terminals is particularly significant because they are small, have low loss power, have characteristics of steady frequency, and have adequate quality factor (Q)[7]. These devices have been subjected to increased requirements due to the mobile network. These requirements include higher electromechanical coupling coefficients and higher operating frequencies that are more significant than GHz.

The design and analysis of one-port multilayer surface acoustic wave (SAW) resonators play a crucial role in modern communication systems, aiming to minimize return loss and enhance overall system performance.Two primary elements, such as the material's velocity and the interdigital structure's (IDT) finger width, significantly impact the working frequency of SAW devices. According to Fu *et al*. (2018)[8], the primary research path that is being pursued is to either enhance the phase velocity of the IDT or reduce the finger width of the IDT. This is being done to improve SAW devices' working frequency. Reducing the width of the IDT structure primarily depends on improving accuracy during the lithography process; nevertheless, doing so will make the process more complex and will be constrained by the limitations of photolithography[9]. The mechanical displacement of the piezoelectric substrate occurs when an AC electric field is given as stimulation, resulting in the phase velocity of the SAW device[10]. The phase velocity of several piezoelectric materials is found to be distinct from one another. The application of different doped piezoelectric substrates such as$LiNbO_3$, $LiTaO_3$, AlN, *etc*. to the design of SAW devices with higher phase velocity of SAW to fulfil the operating frequency requirement. On the other hand, this approach cannot significantly increase the phase velocity[11]. This issue is resolved by the formation of a new structure that is composed of

*Corresponding author: (E-mail: basudeb.ece@nitjsr.ac.in)

layers. By depositing a single layer or multiple layers of piezoelectric thin films on the surface of a high-speed piezoelectric substrate, the SAW's electromechanical coupling coefficient and phase velocity can be improved concurrently[12]. Furthermore, the multi-layer structures can completely utilise their advantages by selecting materials with different features. In addition to enhancing and expanding the functionality of SAW devices, there is also the possibility of improving their compatibility with the working environment and the stability of their operation. Consequently, developing high-frequency operated and high-performance SAW devices will inevitably lead to a multi-layer SAW structure[13]. Murata *et al*.[14] manufactured IF and RF filters and duplexers that operate at 1280 MHz.

For this work, a multi-layered SAW resonator structure of Aluminium, Lithium niobate, and Si is constructed and analysed using the finite element approach. First, a two-dimensional model of the fundamental unit structure is created, and then the structure's modal properties and admittance characteristics are determined. The thickness of the piezoelectric layer and the electrode thickness are optimised based on this information. Following the completion of the design process, a complete two-dimensional resonator structure is created at the desired operating frequency.

2 Principle of the Layered Structure

Multilayered SAW devices have been extensively researched due to their additional properties compared to SAW in piezoelectric media[13]. In multilayer structures, the phase velocity of SAW is influenced by factors such as the thickness of each layer, direction of propagation, frequency of the applied voltage, and the metallisation of the surface and interface. The device's performance can be altered by changing the film's thickness, the substrate's composition, and the electrode's configuration[15]. The device's speed is influenced by its frequency, and surface acoustic waves (SAW) in a multi-layer structure exhibit wave dispersion. The high phase velocity of SAW in multi-layer structures facilitates the development of devices operating at frequencies in the tens of gigahertz range[16]. Multi-layer structures support multiple modes of SAW, and the most optimal mode can be determined through analysis.

Multi-layered SAW devices have an additional substrate layer that establishes the essential characteristics of the SAW propagation and offers mechanical support. It controls the wave velocity and affects the overall performance of the resonator[17]. The IDT electrodes, which translate electrical inputs into mechanical displacements and vice versa, are then formed by depositing thin film layers on the substrate. These layers are carefully engineered to guarantee accurate matching of impedance and effective transfer of energy[18]. Adding more layers could enhance the resonator's filtering capabilities and customise its frequency response. These could consist of reflector layers to improve acoustic wave reflection and guiding layers to focus acoustic energy. High-performance signal filtering with features like sharp roll-off, high selectivity, and low insertion loss can be achieved by the multi-layered SAW resonator by carefully choosing and optimising each layer's material composition, thickness, and geometry—attributes in addition to SAW's traits in piezoelectric media.

Silicon has a high acoustic velocity, so SAW travel quickly through silicon substrates. This property is critical for high-frequency operation and efficient signal filtering in SAW resonators[19]. Since silicon has a low acoustic loss, SAWs propagate through the material with little attenuation. Sharper and more focused frequency filtering in SAW resonators is made possible by high Q-factor (quality factor) resonance, which is only possible with low acoustic loss[20]. Silicon-based SAW resonators on the same semiconductor chip can easily integrate with electronic components and circuits, such as amplifiers, filters, and transducers. This integration simplifies system design, reduces component count, and enhances overall performance and miniaturisation[21].

Lithium niobate has a high piezoelectric coefficient, which means it efficiently converts electrical input into mechanical vibrations and vice versa. This property is essential for creating and detecting surface acoustic waves in SAW resonators. High piezoelectric coefficients enable strong interaction between the electrical and mechanical domains, resulting in effective signal filtering[21]. In a study by Fu *et al*. (2018), it was found that the reflecting grating's reflectivity is at its maximum when $a/\lambda = 0.25$, meaning that the metallisation ratio (a/p) is 0.5.In this paper, the one-port SAW resonator's operating frequency is 1300MHz.Here, the velocity ‘v’ of the material is 7800 of the layered device, which can be found in reference[22] using the formula.

$$v = \lambda f \quad \text{... (1)}$$

From the above equation, the wavelength is found to be $6\mu m$.

The available wavelength is $6\mu m$, and the aluminium 'Al' metal is used as IDT with pitch p=$\lambda/2$. The spacing between electrodes d and electrode width are both equal. The SAW in the Si/$LiNbO_3$ structure is mode 1, as indicated by the dispersion curve relationship in [176] and the phase velocity selection mentioned earlier. The comparative thickness $h_{LiNbO_3}k$ of the piezo layer is approximately 1.6, where k=$2\pi/\lambda$. As a result, $h_2$is found to be the thickness of the piezo layer $LiNbO_3$. Given that the majority of the descending energy of SAW mainly concentrates in 1-2 wavelengths[18].

3 Design and Meshing of the Proposed Device

Figure 1 shows the proposed multi-layered SAW resonator consisting of Al, $LiNbO_3$, and silicon oxide and its dimensions are shown in Table 1.

Aluminium has excellent electrical conductivity, which is required for efficient signal transmission and minimal energy loss in the electrodes and IDTs of SAW devices. $LiNbO_3$ is a crucial material for SAW resonators due to its excellent piezoelectric, acoustic, and mechanical properties. $LiNbO_3$ has a high piezoelectric coupling coefficient, so it can efficiently convert electrical inputs into mechanical outputs and vice versa. This efficiency is crucial for the performance of SAW resonators, enabling strong signal generation and detection. Silicon oxide is used in SAW resonators because it controls acoustic wave propagation, maintains temperature stability, improves piezoelectric properties, gives electrical isolation, and protects the device from physical and chemical damage.

Its mechanical properties and compatibility with silicon-based technology make silicon oxide essential in designing and manufacturing high-performance SAW resonators. Fig. 2 represents the mesh of the proposed one-port SAW resonator. In this structure, the Finer size of the Free Triangular Meshing type has been adopted to simulate the structure[23].

Boundary conditions as given in Table 2, play a crucial role in the design and functioning of SAW devices. SAW devices, which include filters, resonators, and sensors, rely on the propagation of acoustic waves along the surface of a material, typically a piezoelectric substrate. Boundary conditions of SAW devices impacted Wave Propagation Control, Impedance Matching, Frequency Stability and Accuracy, Energy Trapping, Device Size and Miniaturization, Reduction of Spurious Modes, and Thermal and Mechanical Stability.

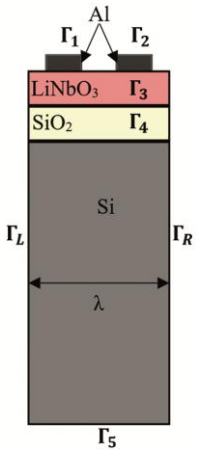

Fig. 1 — Represents the model of the proposed one-port SAW resonator

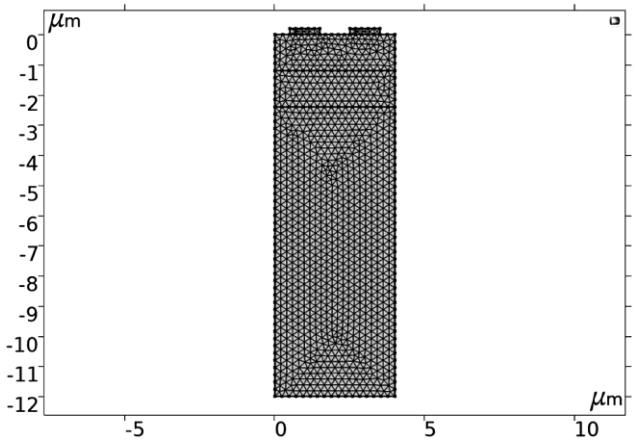

Fig. 2 — Meshing of the proposed one port multi-layer SAW resonator

Table 1 — Dimension of the proposed device

Wavelength (λ)(μm)	Pitch (P)(μm)	a/p	Al (μm)	$LiNbO_3$ (μm)	SiO_2 (μm)	Si (μm)
4	2	0.5	1×02	4×1	4×1	4×10

Table 2 — Boundary condition used for simulation

	Boundary Conditions	
	Electrical	Mechanical
Γ_1,Γ_2	Potential/ Ground	Free
Γ_3	Continuity	Free
Γ_4	Continuity	Free
Γ_5	Ground	Fixed constraint
Γ_L,Γ_R		Periodic condition

3.1 Comparison with BAW Devices

3.1.1 Mode of Wave Propagation

While SAW devices rely on wave propagation along the surface, BAW devices utilize wave

propagation through the bulk of the material. However, boundary conditions in both types of devices are critical in determining the resonant frequencies, mode shapes, and overall performance.

3.1.2 Frequency Range and Applications

BAW devices typically operate at higher frequencies and are more suited for applications requiring high power handling and low insertion loss, such as in mobile communications. The boundary conditions in both SAW and BAW devices are designed to optimize these specific performance characteristics.

4 Modelling and Simulation

This paper simulates and analyses the structure using COMSOL Multiphysics. In COMSOL, coupling the electrical and structural domains can represent the relationship between the material strain and the dielectric constant when strain is constant or material stress and dielectric constant when stress is constant. A strain and a stress charge are the two charge equations typically used[24-25]. The quasi-static equations for modelling piezoelectric devices comprise the structural equation connecting Newton's and Gauss's laws. Differential equations can be used to describe the propagation of SAW. These equations must be solved with design problems, including the device's complexity, the material's performance, and boundary conditions. Determining the numerical solution to the related differential equation can be accomplished using the finite element method. The strain (S), stress (T), electric displacement (D), and electric field (E) of piezoelectric materials can be determined using the following equation[22]:

$$T_{ij} = c^{E}_{ijkl} S_{kl} - e_{kij} E_k \quad \text{... (2)}$$

$$D_i = e_{ikl} S_{kl} + \varepsilon^{S}_{ij} E_k \quad \text{... (3)}$$

In this equation, T_{ij} represents the stress vector,C^{E}_{ijkl} represents the elastic matrix (in terms of N/m2),e_{ikl} represents the piezoelectric matrix (in terms of C/m^2),e_{ij} represents the dielectric constant matrix (in terms of F/m), E_k represents the displacement vector (in terms of V/m), S_{kl} represents the strain vector, and D_i represents the electric displacement (in terms of C/ m^2). One can obtain potential V by resolving the Maxwell and Newton equation, which are as follows:

$$\rho \frac{\eth^2 u_i}{\eth t^2} = C_{ijkl} \frac{\delta^2 u_i}{\delta x_j \delta_l} + e_{kij} \frac{\delta^2 u_i}{\delta x_j \delta x_l} \quad \text{... (4)}$$

$$e_{ijl} \frac{\delta^2 u_l}{\delta x_j \delta x_l} - \varepsilon_{jk} \frac{\delta^2 \phi}{\delta x_j \delta x_l} = 0 \quad \text{... (5)}$$

In which i,j,k =1,2 and 3 respectively.

5 Results and Discussion

Figures 3 & 4 show the total displacement profile at resonance and anti-resonance conditions containing red, yellow, and blue, showing the displacement of the particle in the device. In this device, maximum displacement occurs on the material's surface, decreasing when the wave travels away from the surface. The maximum displacement of the particle is 3mm at resonance frequency 802 MHz. In the silicon (Si) layer, the particle's displacement is zero in Figs 3 & 4.

When a metal film covered the piezoelectric material, the electrode mass loading phenomena occurred because changes in the electrode's thickness directly affected the admittance of the SAW resonator[23]. The designed SAW resonator experienced minimum impedance and losses when the admittance reached its maximum value, resulting in the maximum amplitude of the Rayleigh wave. Thus, different values of electrode thickness were used to

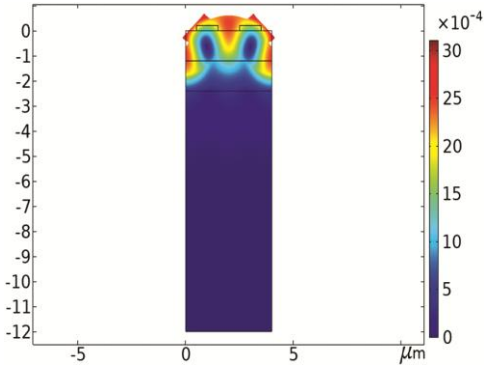

Fig. 3 — Displacement profile of one port multilayer SAW resonator at resonance condition

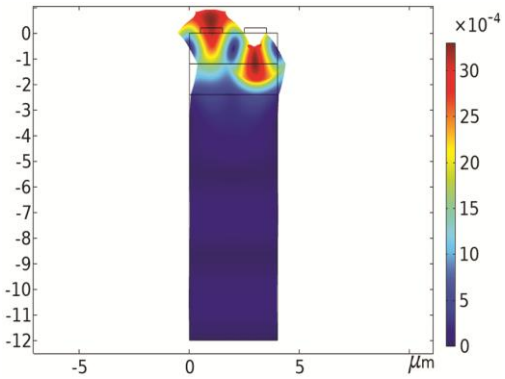

Fig. 4 — Displacement profile of multilayer SAW resonator at anti-resonance conditions

analyse the connection between resonator admittance and electrode thickness.

The plotted results in Fig. 5 of the parametric simulation at roughly 190 nm electrode thickness show that the admittance reached relatively high levels. A more exact sweep was carried out with this thickness, stepping 10 nm between 180 and 220 nm.

First, the frequency ranged between 800 MHz and 820 MHz, and the electrode thickness between 0.010 λ and 0.025 λ in steps of 0.0025 λ. In Fig. 6, the amplitude exhibits the highest possible amplitude when the electrode width is 0.02λ, and the frequency is 816MHz, respectively. The admittance is 0.00020 mho at a frequency of 816MHz.

Figure 7 represents the reflection coefficient of one port multi-layer SAW resonator by variation of electrode width. The S_{11} parameter represents the ratio of the reflected signal to the incident signal of the device. It is expressed in logarithmic form, where a smaller S11 value indicates less signal loss within the device. Conversely, the S11 curve exhibits a greater slope, indicating that the SAW resonator possesses a higher Q value. In Fig. 7, the reflection coefficient of 190 nm electrode width is less than that of other electrode widths.

A lower reflection coefficient indicates less reflection and better signal transmission efficiency. For example, lower reflection coefficients are preferred in telecommunications to minimise signal loss. In Fig. 5, the width of the electrode is 0.010λ, which indicates the reflection is less than one compared to another electrode width. Hence, in my simulation, I have taken the width of the electrode as 0.010λ, which indicates a brown colour in Fig. 8.

Figure 9 compares a quality factor vs frequency at different electrode heights and values are given at Table 3. The quality factor increases with the height of the electrode. When the electrode width is 200nm, the maximum quality factor is achieved in the proposed device. After 200 nm, the quality factor is

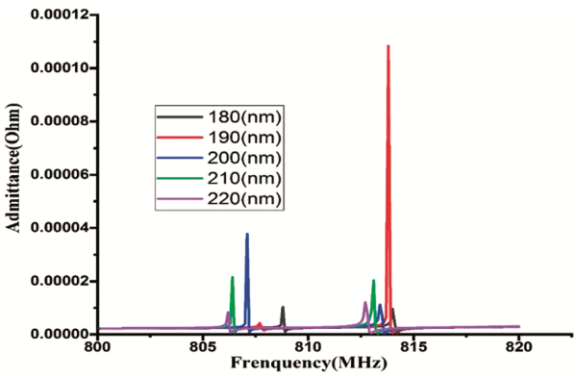

Fig. 5 — The admittance characteristics (Y11) of the resonator with a variation of frequency Electrode thickness from 180 nm to 220 nm

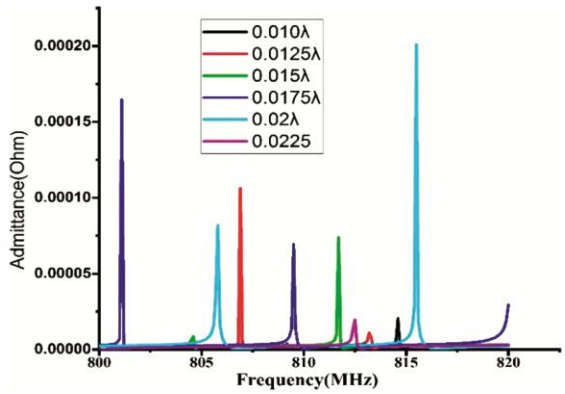

Fig. 6 — Admittance curves for different electrode thicknesses ranging from 0.010 λ to 0.025 λ

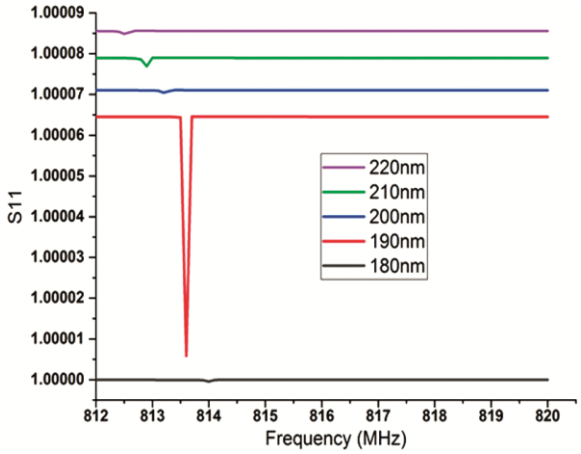

Fig. 7 — Reflection coefficient of various thicknesses of the electrode at different frequencies

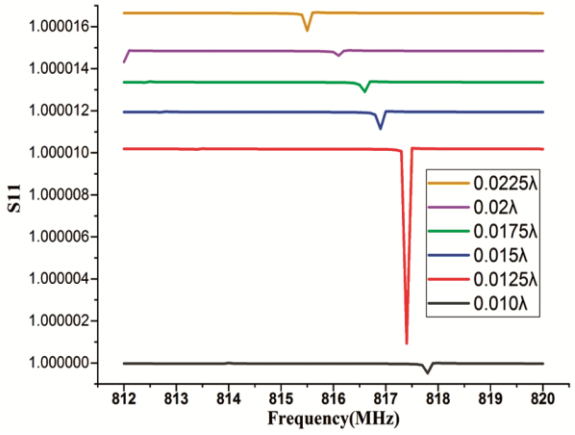

Fig. 8 — The reflection coefficient of various thicknesses of electrodes depends on wavelength at different frequencies

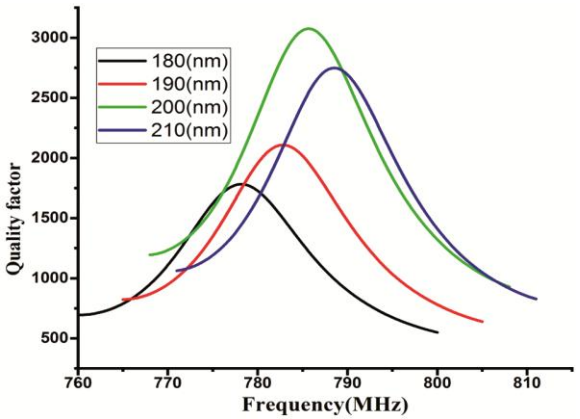

Fig. 9 — Compares the quality factor concerning frequency at different electrode widths

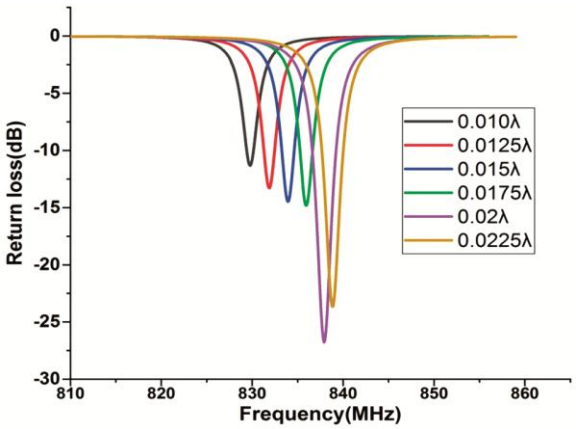

Fig. 10 — Represent return loss as a function of electrode thickness

Table 3 — Compare quality factors at different Aluminum width

Width of electrode(nm)	Quality factor	Frequency(MHz)
180	1781	778
190	2107	782
200	3075	785
210	2748	788

decreasing. From Table 2, the optimum value of the thickness of the electrode is 200nm.

The return loss graph is vital for understanding the performance of a single-port SAW resonator. It indicates the resonant frequency, impedance matching quality, bandwidth, and overall device efficiency in filtering or producing specific frequencies. A high return loss at the resonant frequency indicates efficient energy transfer and optimal resonator performance.

Figure 10 represents return loss by variation in the thickness of the electrode. When the electrode is 0.010λ, the return loss is close to 0dB compared to another electrode width. It means poor impedance matching and high reflection of the signal. High return loss (27dB) occurs at 838MHz when the electrode width is 0.02λ. A high return loss indicates that only a tiny fraction of the signal is reflected, signifying a good impedance match between components. This is advantageous in most applications.

6 Conclusion

In this work, we introduced a One-Port multi-layer SAW resonator and analysed many features, including the quality factor, admittance, and impedance ratio: reflection coefficient and insertion loss. Improving the performance of the proposed multi-layered resonator by reducing its return loss enhances efficiency by minimising the power of the reflection. This work optimised the height of the electrode and found the insertion loss of the proposed device, which was -27dB.The proposed device has enhanced performance characteristics that are suitable for various communication system applications, including wireless networks, radar systems, and satellite communications.

References

1 Mujahid A & Dickert F L, *Sensors* 17 (2017) 2716.
2 Aissa K A, Achour A, Elmazria O, Simon Q, Elhosni M, Boulet P, Robert S & Djouadi M A, *J Phys D: Appl Phys*, 48 (2015) 145307.
3 Zubair A M, Jeoti V, Karuppanan S, Malik A F & Iqbal A, *Sensors*, 18 (2018) 1687.
4 Burkov S I, Olga P Z, Sorokin B P, Turchin P P & Talismanov V S, *The J Acoust Soc Am*, 143 (2018) 16.
5 Qing F Y, Luo J K, Nguyen N T, Walton A J, Flewitt A J, Zu X T, Li Y, *et al.*, *Progress Mater Sci*, 89 (2017) 31.
6 Fu S, Wang W, Qian L, Li Qi, Lu Z, Shen J, Song C, Zeng F & Pan F, *IEEE Electron Dev Lett*, 40 (2019) 103.
7 Fu C, Ke Y, Quan A, Li C, Fan X, Ou J & Luo J, *Surf Coat Technol*, 363 (2019) 330.
8 Sahoo G, Turuk B K, Behera B, *AIP Conf Proc*, 2341 (2021) 020012.
9 ChKaletta Udo, Santos P V, Wolansky D, Scheit A, Fraschke M, Wipf C, Zaumseil P & Wenger C, *Semicond Sci Technol*, 28 (2013) 065013.
10 Qian L, Li C, Li M, Wang F & Yang B, *Appl Phys Lett*, 105 (2014).
11 Luo J, Quan A, Fu C & Li H, *J Alloys Compd*, 693 (2017) 558.
12 Turuk B K & Behera B, *Mater Today: Proc*, 56 (2022) 883.
13 Maouhoub S, Aoura Y & Mir A, *Diamond Relat Mater*, 62 (2016) 7.
14 Mortet V, Elmazria O, Nesladek M, Assouar M B, Vanhoyland G, Haen J D, Olieslaeger M D & Alnot P, *Appl Phys Lett*, 81 (2002) 1720.
15 Behera B & Nemade H B, *Proc Eng*, 144 (2016) 1411.
16 Vincent M, Williams O A & Haenen K, *Physica Status Solidi(a)*, 205 (2008) 1009.

17 Turuk B K & Behera B, *Eng Res Express*, *IOP Publishing*, 6 (2024) 022302.
18 Naumenko N F, *Ultrasonics*, 95 (2019) 1.
19 Ioannis N, Hallil H, Tamarin O, Dejous C & Rebière D, *2016 31st Symposium on Microelectronics Technology and Devices (SBMicro)*, Belo Horizonte, Brazil, (2016) 1.
20 Ritter F, Hedrich J, Deck M, Ludwig F, Shakirov D, Rapp B E & Länge K, *Proc Technol*, 27 (2017) 35.
21 Ro R, Chiang Y-F, Sung C-C, Lee R & Wu S, *IEEE Trans Ultrason Ferroelect Freq Control*, 57 (2009) 46.
22 Ro R, Lee R, Lin Z X, Sung C C, Chiang Y F & Wu S, *Thin Solid Films*, 529 (2013) 470.
23 Behera B & Nemade H B, *Simulation*, 95 (2019) 117.
24 Turuk B K & Behera B, *Ferroelectrics*, 615 (2023) 132.
25 Turuk B K & Behera B, *Ferroelectrics*, 583 (2021) 33.